Materials Research. 2017; 20(3): 688-701
DOI: http://dx.doi.org/10.1590/1980-5373-MR-2016-0459

Simulation of CP-Ti Recrystallization and Grain Growth by a Cellular Automata Algorithm: Simulated Versus Experimental Results

Rodrigo José Contieri[a]*, Marcelo Zanotello[b], Rubens Caram[c]

[a] *School of Applied Science, University of Campinas, Limeira, SP, Brazil*
[b] *Center for Natural and Human Sciences, Federal University of ABC, Santo André, SP, Brazil*
[c] *School of Mechanical Engineering, University of Campinas, Campinas, SP, Brazil*

Received: June 16, 2016; Revised: November 01, 2016; Accepted: March 09, 2017

The application of cellular automata in materials science requires the conversion of the automata's rules and abstract general properties to rules and properties associated with the material and phenomena under study. In this paper we propose a model which uses cellular automata to simulate recrystallization and grain growth during isothermal and non-isothermal treatments of cold worked polycrystalline materials. The algorithm's spatial and temporal scaling is based on known experimental results for recrystallization and grain growth in highly cold-worked commercially pure titanium grade 2. In the recrystallization, the best agreement between experimental and computational results in terms of the process kinetics and the average diameter of recrystallized grains is obtained from a nucleation model that considers the temperature-dependent nuclei formation rate. In the simulation of grain growth after primary recrystallization, the results indicate the normal growth of an equiaxed grain structure whose kinetics and dimensions are comparable to those observed experimentally.

Keywords: *recrystallization, grain growth, cellular automata, titanium*

1. Introduction

Processes and natural phenomena are usually modeled by partial differential equations that govern the continuous spatial and temporal evolution of the relevant quantities that describe the system under study. In most cases, possible solutions to such equations are only obtained numerically, with the differential formulation transformed, for example, into a finite difference scheme to be implemented computationally using an appropriate algorithm. Alternatively, it is possible to describe the spatiotemporal evolution of complex systems by models that are implemented using algorithms involving cellular automata[1,2]. A cellular automaton consists of a grid of cells, also called sites, which is arranged in one, two or three dimensions and may present various geometric shapes such as squares, rectangles, hexagons or cubes. Each cell is characterized by a finite number of attributes or properties. The set of attributes of a cell defines its state. The cellular automaton evolves in almost imperceptible steps over time, so that at each level of time, the properties associated with each cell are updated according to well-defined transformation rules. The rules determine the new values of the properties to be assigned to a particular site, considering the site's past values and the past values of the properties of sites located in its neighborhood. Among the several possibilities for defining the neighborhood of a given cell, the ones most commonly used are those proposed by von Neumann and Moore, which consider, respectively, the 4 and 8 nearest neighbors for a lattice of square cells. Transformation rules, which may be deterministic or probabilistic, are applied simultaneously to all the cells of the grid at each level in time[1,2]. With these characteristics, cellular automata provide a discrete method to directly simulate the evolution of complex dynamic systems that contain large numbers of similar components, based on short or long-range local interactions among their elements. This enables useful models to be constructed for numerous investigations in physics, chemistry, biology, mathematics, and computer science, thus representing an alternative to the formulation of physical phenomena by partial differential equations[3].

The use of cellular automata (CA) in materials science is feasible by converting the rules and abstract general properties of automata into rules and properties associated with the material and phenomena under study. These rules are determined by the application of physical laws or experimentally proven results. The cells in the grid can represent atoms, clusters of atoms, segments of dislocations or small amounts of crystalline material with some degree of orientation. Raabe[4] points out that the versatility of the formulation by CA in the simulation of microstructural transitions, especially in recrystallization, grain growth and phase transformations, is due to the algorithm's flexibility, which enables it to consider a wide range of state variables and transition rules. In simulations of recrystallization and grain growth by CA, the influence of energies and mobilities of grain boundaries, driving forces and preferential crystallographic orientations can be considered to determine their kinetics, textures and

* e-mail: rodrigo.contieri@fca.unicamp.br

microstructures on realistic temporal and spatial scales, allowing for quantitative predictions and comparisons with experimental data. It should be emphasized that in such simulations the spatial dimensions and time interval employed are not intrinsically calibrated by a characteristic physical length or time scale, so that the CA simulation of a continuous system requires the definition of elementary units and rules of transition that adequately reflect the behavior of the system at the desired level, as pointed out by Raabe[4].

Hesselbarth and Göbel[5] were pioneers in introducing a model to simulate the recrystallization kinetics based on cellular automata algorithm. From an initial uniform structure in which all the cells were in a "non-recrystallized" state, these authors imposed a nucleation rate on the system, so that the state of some randomly selected cells was converted to "recrystallized", characterizing them as new phase nuclei. These nuclei grew through the transition from their neighbors to the "recrystallized" state, according to specific rules. Evaluating the effect of different definitions of neighborhoods, the authors showed that the model reproduces the transformation kinetics in agreement with the theory of Johnson, Mehl, Avrami and Kolmogorov (JMAK theory), with the curve of the fraction transformed as a function of time, showing non-sigmoidal behavior at each temperature in the description of a homogeneous recrystallization process. Deviations with respect to JMAK theory were obtained with different transition rules for nuclei growth, simulating conditions of heterogeneous recrystallization.

Despite the success of the model developed by Hesselbarth and Göbel[5] in reproducing the behavior predicted by JMAK theory, the recrystallization kinetics was not calibrated to the real time of the process, nor was any spatial scale attributed to the resulting microstructure. Stiko[2] and Davies[6] modified the rules of transition between neighboring cells using growth models related to a realistic time scale. Others researchers investigated the influence of initial microstructure topologies on the kinetics of static recrystallization in simulations by CA[1,2,7], and static recrystallization in cold-worked copper[8] and in iron[9] were recently simulated by a CA algorithm. Dynamic recrystallization models using cellular automata were proposed by Goetz and Seetharaman[10], Qian[11], Ding[12] and Yazdipour[13] to simulate the microstructural evolution of materials during thermomechanical processing.

In simulations of grain growth, Geiger *et al.*[14] developed a CA model that involves the determination of an energy barrier for cellular energy-dependent transitions of grain boundaries, which in turn depends on the difference in orientation between adjacent grains. He, Ding and co-authors studied the morphology and kinetics of grain growth in two[15] and three dimensions[16] by computer simulation, using a model of cellular automata based on the principle of minimum energy. Through a balance between the system's thermodynamic energy and the energy associated to grain boundaries, the algorithm they developed promotes the transition of a cell of the automaton, ensuring the reduction of the system's power. Raghavan and Sahay[17] proposed a cellular automaton model that estimates the grain boundary curvature to evaluate the driving force governing the process of grain growth in aluminum.

Based on a two-dimensional cellular automata algorithm, Rappaz and Gandin[18] proposed a model for simulating the formation of grain structures in solidification processes. The model includes the mechanisms of heterogeneous nucleation, both at the liquid's interface with the mold walls and inside the liquid metal, and of dendritic grain growth in preferred directions. The columnar-to-equiaxed transition and the equiaxed grain overlay were simulated based on the effects of alloy concentration and cooling rates on the resulting microstructure observed experimentally. Nastac and Stefanescu[19] combined the effects of solute micro-segregation and super-cooling in their stochastic model for simulating the formation of micro-structural solidification using cellular automata. Zhu and Hong[20] developed a cellular automata model to simulate eutectic growth, specifically the formation of lamellar morphologies in directional solidification conditions. Effects of growth rate on volume fraction, and consequently on the lamellar spacing between eutectic phases, were observed in two-dimensional domains.

The aim of this paper is to develop a cellular automata algorithm to simulate recrystallization and grain growth phenomena in isothermal and non-isothermal conditions, analyzing the results in the light of experimental results for these phenomena in highly cold-worked commercially pure titanium grade 2 [21]. This model combines several aspects of the phenomena reported in previous works involving isothermal simulations, and also contributes by proposing its extension to a non-isothermal simulation. A calibration of the model's spatial and temporal dimensions is suggested based on experimental data that allow the kinetics of primary recrystallization and the evolution of average grain size in the growth stage of the material to be analyzed quantitatively. Three possible mechanisms of nucleation in the primary recrystallization stage are proposed, and an investigation is made to determine which of these mechanisms yields results closest to the experimental results. An analysis is made of situations simulating both isothermal treatments and Differential Scanning Calorimetry (DSC) experiments in which the temperature varies according to a given time rate.

2. Kinetics of Recrystallization and Grain Growth

The plastic deformation of a sample of polycrystalline metallic material at low temperatures compared to its melting temperature, also known as cold working, produces variations in its properties and microstructure, such as changes in the grain's shape, hardness, increased dislocation density, corrosion resistance, and thermal and electrical conductivities.

The reason for these variations is that although most of the energy involved in the cold working process is dissipated as heat, a considerable part of energy, called strain energy, is stored in the material. The basic mechanism that causes deformation in metals consists in the generation and motion of dislocations that favor relative displacements between the atomic planes. Strain energy is associated with the presence of tensile, compression and shear zones around the dislocations generated[22].

The original properties and structure can be restored by subjecting the material to an appropriate heat treatment at elevated temperatures. This treatment gives rise to recovery and recrystallization phenomena, which may be followed by grain growth and which cause the energy stored during cold working to be partially or totally eliminated. Due to strain energy, cold-worked material is in a higher state of energy than prior to its deformation. Hence, its condition of equilibrium is metastable, enabling its possible transition to a more stable state in favorable thermodynamic conditions involving certain types of activation energy. Recrystallization consists of the formation of a new set of non-equiaxed grains of low dislocation density which are characteristic of the condition prior to the cold working process. The driving force to produce this new grain structure is the difference in the material's internal energy in its non-cold worked and cold-worked states that results from the elimination of dislocations. Thus, recrystallization and grain growth constitute key topics in physical metallurgy, and are relevant to both the theory and processing of metallic materials[22].

The kinetics of primary recrystallization is determined by the thermal activation of nucleation mechanisms and nuclei growth, which control the progress of the microstructure during the heat treatment. However, according to Rios and coauthors[30], the final size of recrystallized grains are more sensitive to applied deformation than the annealing temperature. The amount of deformation affects the rate of recrystallization, that influences the amount of energy stored and consequently the formation of new nuclei or recrystallized grains. The quantitative description of homogeneous recrystallization kinetics is usually based on JMAK theory, which results in an equation such as[22]:

$$X(t) = 1 - \exp(-At^n) \qquad (1)$$

In Equation 1, known as Avrami's equation, X(t) is the fraction of recrystallized material as a function of time "t" of the heat treatment, "n" is the Avrami exponent and "A" is a constant related to the characteristic time of recrystallization. To obtain Equation 1, we consider the random distribution of nucleation sites throughout the microstructure and the fact that newly formed nuclei grow steadily until they impinge on other growing nuclei (*impingement*). The Avrami exponent is determined by Equation 2[22]:

$$\ln\left[\ln\left(\frac{1}{1-X}\right)\right] = \ln A + n\ln t \quad (2)$$

Measuring the recrystallized fraction as a function of treatment allows for the construction of a graph associated with Equation 2, in which the slope equals "n". This procedure is called an "Avrami plot". Further important detail of JMAK equation concerns about their generalization to heat treatment in which temperature is a function of time. In such cases, the recrystallization kinetics when evaluated using isothermal conditions is not straightforward since each step depends on the temperature. According to some authors[22,27,31], the temperature dependence of the nucleation arises from the dependence of the static nucleation process that is thermally activated and therefore correlates with another dependence, the growth mobility. It is then sufficient to use, in place of parameter A (equation 1), a function as A(T(t)); therefore describing the evolution of temperature with time, to update the temperature dependent parameters in the nucleation and growth model at each time step. Briefly, the temperature dependence, provided by the rate of heating of the material to the annealing temperature can affect the rate of recrystallization.

From the metallurgical point of view, normal grain growth can be defined as the uniform increase in average grain size that occurs during the heat treatment of a polycrystalline aggregate after the completion of primary recrystallization. The kinetics of grain growth can be expressed, in terms of the evolution of the grain diameter "D", according to Equation 3.

$$D^m - D_0^m = Kt \qquad (3)$$

The growth exponent "m" can be evaluated by constructing a graph of the logarithm of average grain size by the logarithm of time for each temperature. In so-called normal growth, the grain size distribution is self-similar, indicating that the average grain size has shifted to higher values during the course of the treatment, but the height of the maximum and standard deviation of the distribution do not change.

3. Simulation Methodology

The program consists of two parts. The first relates to primary recrystallization, which includes the nucleation and growth of recrystallized nuclei until the original deformed matrix is completely replaced by new grains devoid of imperfections, reducing the volumetric energy density stored in the system during its cold working process, mostly in the form of dislocations. The second part simulates the growth of recrystallized grains during further heat treatment to minimize the energy of the system by reducing the interfacial energy density associated with grain boundaries.

3.1. Model for primary recrystallization

The fundamental mechanisms involved in primary recrystallization are nucleation and nuclei growth. The details of the nucleation process will not be considered, as

is the case of most of the recrystallization and grain growth simulation studies reported in the literature. In simulations, a nucleus occupies a cell. Hence, the cell size must reflect the approximate dimensions of a real nucleus. From a practical standpoint, this precludes the use of a single length scale to computationally simulate phenomena that occur on significantly different scales, as in the case of nuclei formation and grain growth until they reach their final average size.

The initial condition for the simulation is a situation in which every cell in the field is in the cold-worked state, showing high dislocation density. This hypothesis is consistent with an experimental situation in which the sample's level of deformation is high, distributing the preferential sites for new grain formation almost uniformly over the material. At the initial time, the state of a number of randomly chosen cells in the cold-worked matrix is changed to the recrystallized state. Although it does not represent a real nucleus formation process, this step of the simulation is usually called nucleation and the term "nucleus" is used to designate a cell of the automata whose state has changed to recrystallized. The value assigned to the state of recrystallized cells is 1, while non-recrystallized cells are assigned a value of 0. In addition to the state which indicates that a cell is recrystallized, each cell has an orientation state "q" that varies from 1 to 256, and an identification state "ide". Cells with same "ide" are part of the same grain. The maximum number of orientations used is justified by Geiger[14] as being sufficient to generate realistic microstructures.

Nucleation was simulated by three basic mechanisms. The first mechanism is site saturation, which involves the simultaneous generation of a certain number of nuclei distributed randomly over the grid only at the initial time. Subsequently, the nuclei grow until they impinge on one another and the process continues until the whole matrix is recrystallized. In the second mechanism, the nuclei appear at a constant rate (nuclei density) during recrystallization until the process is complete and the entire matrix has been transformed. In this type of nucleation, the rate is defined by imposing on the system the number of nuclei that arise at each step in time. Finally, the third nucleation mechanism considers the temperature and activation energy involved in the process by means of Equation 4, which calculates the percentage of nucleated cells at a given moment. In Equation 4, Qn is the activation energy for nucleation, R is the universal gas constant, T is the temperature of heat treatment, and N_0 is a pre-exponential factor independent of temperature[22].

$$N(t) = N_0 \exp(-Q_N/RT) \quad (4)$$

In each case, the nuclei were generated at randomly selected sites in the matrix, since an initial condition is assumed in which the dislocation density is uniform throughout the system. The recrystallized nuclei, at a certain moment, grow until the matrix is completely filled with small new grains free of imperfections. The growth rate of such nuclei, expressed in terms of driving force "p" for primary recrystallization and mobility "m" of the interface established between a region (in theory) free of imperfections and another with a high density of imperfections, is written as[23]:

$$v = mp \quad (5)$$

The mobility of the boundary is given by:

$$m = m_o \exp(-Q_A/R \cdot T) \quad (6)$$

The driving force for primary recrystallization, ignoring the remaining dislocation density, is:

$$p = \frac{1}{2}\rho G b^2 \quad (7)$$

In Equations 6 and 7, "m_o" is a constant, "Q_A" is the activation energy for the movement of grain boundaries, "R" is the gas constant, "T" is the temperature, "G" is the shear modulus, "b" is the modulus of the Burgers vector, and "ρ" is the dislocation density.

The nucleus thus generated will have probability of growth which, according to Davies[6], can be written as:

$$P_{CG} = \frac{\int v \cdot dt}{S_{AC}} \quad (8)$$

In Equation 8, "S_{AC}" is the size of the cell and "v" the velocity of the interface given by equation 5. If a cell has at least one nucleus in its neighborhood, it will have a certain probability to recrystallize. Thus, if a random number located at the interval [0,1] provided by the RAND routine in the Fortran 90 program is greater than or equal to the probability of growth, the state of the cell neighboring the nucleus is changed to recrystallized, which is equivalent to the movement of the boundary through a cell. Otherwise, the cell in question remains in the non-recrystallized state.

3.2. Model for grain growth

In the simulation of grain growth, the orientation and identification stages used in the nucleation step are maintained and a new "E_B" state is assigned to each cell, characterizing the boundary energy between adjacent cells which is generated by the difference in their orientations. This portion was not considered in the calculation of the driving force in the primary recrystallization stage because it is generally about three orders of magnitude smaller than the stored strain energy, according to Gottstein[22]. The grain growth in the algorithm is governed by the change in orientation of the cells located in a boundary region. The transition rule for the orientation of a particular cell is based on the reduction of its interfacial

energy. For each cell, denoted by "i", we initially calculate its interfacial energy E_{Bi} according to Equation 9.

$$E_{Bi} = \sum_{j=1}^{8} \gamma_{ij}(1 - \delta_{qi,qj}) \quad (9)$$

In our case, the number of neighbors equals 8, due to Moore's definition of neighborhood, which was used in the simulations, while δ_{ij} is the Kronecker delta equal to 1 if i = j, (cell i has the same orientation as the cell j), and equal to 0 otherwise (cell i has a different orientation of cell j). The boundary energy γ_{ij} between two adjacent cells is provided by Wolf's[24] adaptation to the equation proposed by Read and Schokley, expressed by Equation 10. Details about permutation between neighboring by Moore´s definition can be found in previous studies of cellular automata algorithm[32,33].

$$\gamma_{ij} = E_0 sen\theta_{ij}[1 - \ln(sen\theta_{ij})] \quad (10)$$

Were E_0 is the maximum grain-boundary energy seen at angle θ_{ij}, that denotes the difference in orientation between cells.

$$\theta_{ij} = \frac{\pi}{2}\frac{|q_i - q_j|}{q_{\max}} \quad (11)$$

Through the field at each time step, the orientation of each cell is provisionally altered by assigning to it the orientation of one of its eight neighbors, and the new boundary energy is calculated. If the interfacial energy presents a decrease, the new orientation given to the cell can be maintained and the transition can be confirmed for the next time level. In the procedure adopted, eight possible final boundary energies are calculated, provisionally attributing to this cell the orientation of each of its neighbors. If the attributions of any of its neighbors' orientations reduce the cell-boundary energy, its original orientation is maintained. If more than one attempt of reorientation results in a decrease in boundary energy, the algorithm attributes to the cell, with a certain probability, the orientation that causes the maximum possible reduction of boundary energy. Thus, the driving force for the migration of grain boundaries is the minimization of the boundary energy between neighboring cells of adjacent grains. Besides reducing the interfacial energy in the boundaries, the model also considers the influence of a potential barrier to be overcome by the cell so that its orientation is altered. This is only possible if there is sufficient heat. This condition is depicted by the mobility of the boundary given by Equation 6, in which the activation energy Q_A is replaced by the activation energy associated with grain growth Q_C.

When the reduction of grain boundary interfacial energy is possible, the change in the cell's orientation will be confirmed through a probability given by a relation similar to Equation 8, in which the driving force for the calculation of interfacial speed now corresponds to the difference in interfacial energy between cells. In short, the transition rule used is: if $\Delta E_B > 0$, the state of the cell is not changed; if $\Delta E_B \leq 0$, the change in the cell's orientation will have a probability of occurrence, minimizing as much as possible the interfacial energy among the cells in question.

4. Results and Discussions

To computationally implement the recrystallization and grain growth model with the cellular automata algorithm, we used a two-dimensional matrix with 300x300 cells. In addition, we used Moore's definition of neighborhood, in which the state of each cell depends on the state of the eight nearest neighbor cells. Periodic boundary conditions were adopted in the domain border and the code was developed based on Fortran 90 programming language. An important aspect of the application of cellular automata is the scaling of time and space. The spatial scaling was performed by attributing a given unit of length to each cell, chosen as 1 mm, as this is a usual scale for measurements of average crystalline grain size in metallic materials[25]. The correlation between a realistic time scale and time step in the simulation by cellular automata (cellular automata step – CAS) was determined based on the measured time for recrystallization in experiments using titanium samples[21]. In the stage of primary recrystallization, each CAS corresponds to 0.5 minutes, and in the grain growth stage the CAS/minute ratio equals 1.0. Some input parameters for the simulation correspond to experimental results regarding the procedures performed for the cold-worked commercially pure titanium grade 2 with 86% reduction in thickness[21], while other parameters are taken from references in the literature. Table 1 lists the values of the parameters used in the developed code.

4.1 Primary recrystallization

In the simulation of primary recrystallization during an isothermal treatment, the temperatures of 873 K, 948 K and 1023 K were considered, which coincide with the experimental treatment temperatures applied to the titanium samples[21]. The mechanisms simulated in this study were site-saturated nucleation, nucleation at a constant rate at any annealing temperature, and nucleation at a temperature-dependent rate. In the site saturation mechanism, in the first moment of the simulation, the status of 2700 randomly selected cells changed to "recrystallized" and, in the course of time, the progress of transformation occurred exclusively through the transition rules between recrystallized and non-recrystallized cells. In the mechanism of nucleation at a constant rate (independent of temperature), the status of 540 randomly selected cells at each instant was changed to "recrystallized", at any temperature at which the heat treatment was performed.

Table 1: Input –parameters for simulation.

Parameters	Values
$Q_N = Q_A$	156.76 kJ/mol [21]
Q_C	110.00 kJ/mol [26]
N_0	5.00 x 10^7
P	6.67 x 10^6 J/m^3 [21]
m_0	5.00 x 10^{-5} [17]
E_0	3000 J/mol [14]
$q_{máx}$	256 [14]
R	8.314 J/mol.K

These values for the initial number of sites whose state was to be altered were estimated by analyzing the beginning of the recrystallization kinetics curve obtained for samples of titanium in differential scanning calorimetry experiments[21]. To simulate site saturation, the transformed fraction was estimated immediately after the level corresponding to the incubation time of the process; while in the mechanism with a constant rate, the estimation was based on the fraction transformed in the early moments recorded. Thus, at the beginning of the simulation, we considered the density of small consolidated grains, ignoring the incubation time associated with nuclei formation. In the third simulation mechanism, the number of cells altered randomly at each instant was determined based on the annealing temperature, using Equation 4.

Figure 1 shows the graphs of the recrystallized fraction as a function of time at each temperature and nucleation mechanism used in the simulations. The graphs show the sigmoidal curves characteristic of recrystallization kinetics, without the time associated with incubation, since it started from a preestablished condition of initial nuclei. It appears that, at a lower temperature, the speed of transformation is lower for the three simulated nucleation mechanisms. The model then reproduces the dependence expected for the processing speed as a function of treatment temperature: the higher the temperature the faster the primary recrystallization.

Figure 2 shows the evolution of the microstructure generated in the simulation of primary recrystallization at a temperature of 948 K in the course of time, with the respective values of the recrystallized fraction "X". This fraction is determined by the ratio between the number of recrystallized cells and the total number of cells in the field at each instant. In the mechanism of site saturation, the transformation speed in the first 4 min is higher than with the other mechanisms. However, with the sequence of isothermal treatment, it is noted that, after approximately 8 min, the recrystallized fraction reaches a value of about 0.95 in all the nucleation cases studied. This higher speed in the case of site saturation is due to the higher nuclei density applied in the first instant of recrystallization. For the other cases, due to the lower initial densities, the recrystallized fractions are

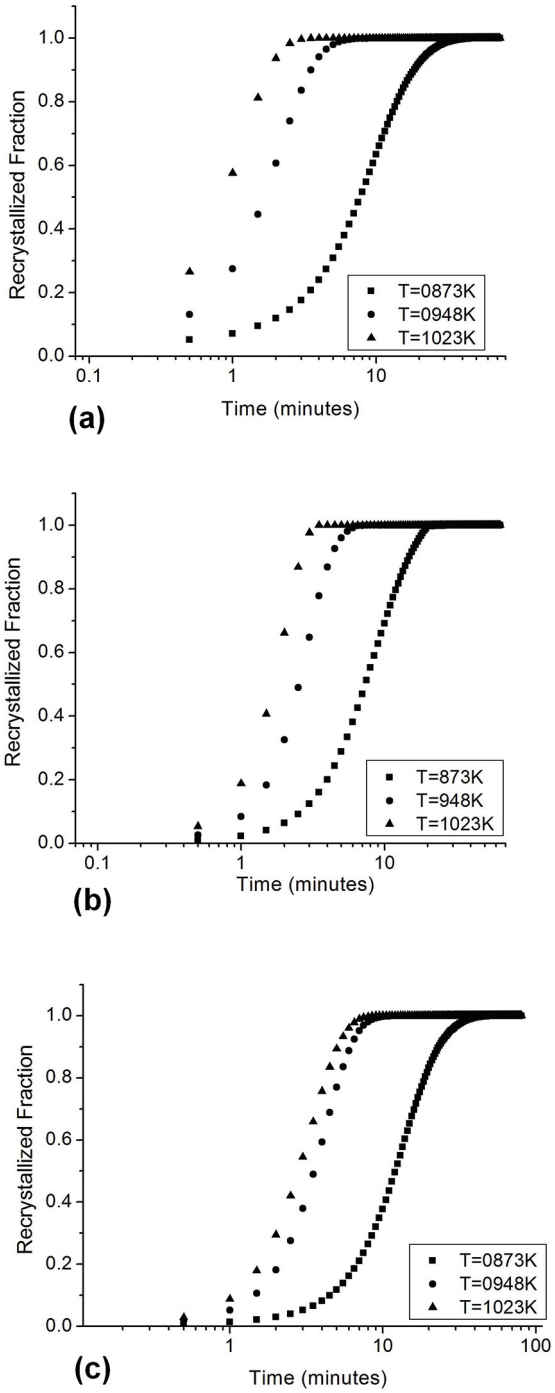

Figure 1: Graphs of the recrystallized fractions as a function of time at temperatures of 873 K, 948 K and 1023 K, and nucleation mechanisms corresponding to site saturation (a), constant rate (independent of annealing temperature) (b), and treatment temperature-dependent rate (c).

lower in the initial instants. Over time, as a greater number of recrystallized cells are nucleated in the mechanisms that involve nucleation rates, the recrystallized fractions in the three simulated mechanisms tend to equalize. The simulated microstructures show that a more refined structure was

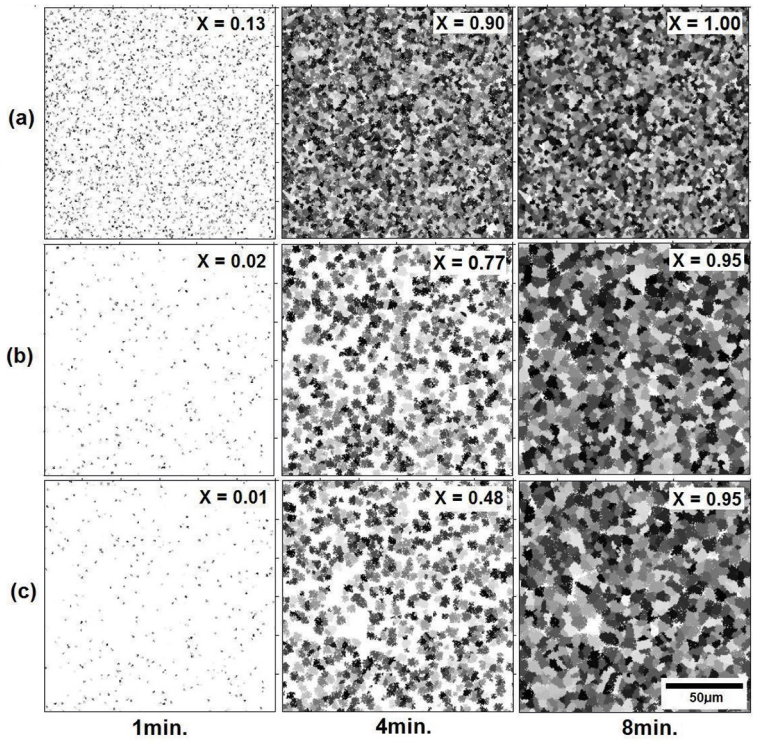

Figure 2: Evolution of primary recrystallization at 948 K for the instants 1, 4 and 8 minutes, simulated by the nucleation mechanisms of: site saturation (a), constant rate (independent of annealing temperature) (b) and treatment temperature-dependent rate (c).

obtained at the end of 8 min for the site saturation, with a larger number of grains showing a lower average size compared with the two other mechanisms.

The effect of annealing temperature on the recrystallization rate is also shown in Figure 3 through Avrami plots. An increase in the Avrami exponent from the lowest to the highest temperature is observed in all the nucleation mechanisms. A decrease in the Avrami exponent in the final moments of the primary recrystallization process, which is highlighted in Figure 3 (b), was observed at almost all the temperatures and nucleation modes, basically due to impingement between growing grains and to the reduction of available sites for the emergence of new recrystallized grains. According to Chun[25], this behavior of the Avrami exponent, which indicates a deviation from the kinetics predicted by JMAK theory, is underpinned in experimental studies on the primary recrystallization in metallic systems. Furthermore, even it is a standard used by many authors, the standard interpretations about nucleation mechanisms are physically simplistic and not surprisingly, the measured n exponent is far from the values expected using these assumptions[27,30,31]. It is however well known that the nucleation rate is non-constant and that recovery takes place concurrently with recrystallisation leading to a non-constant driving force and therefore to a non-constant growth rate. In consonance with these observations, for low temperatures, where the recovery phenomenon becomes dominant, the divergence of the coefficient n with the theory (n=2) is increased.

Table 2 compares the simulated values of recrystallization time and the experimental values obtained by analyzing the softening curves of the samples' microhardness and micrograph measurements taken at each temperature of isothermal treatment[21]. In the simulations, the recrystallization time was determined as the time required for the recrystallized fraction to become (approximately) equal to 1. Specifically, we considered the value of the fraction X = 0.999 as a criterion to define the simulated recrystallization time.

The results of simulated recrystallization times are consistent with the corresponding values measured experimentally, especially for the mechanism of nucleation with temperature-dependent rate, indicating that this seems to be the mechanism that best describes the phenomenon.

As for the morphology of the microstructures generated by simulation at the end of primary recrystallization, Figure 4 shows the formation of an equiaxed grain structure distributed uniformly over the entire grid in the three nucleation cases studied. The average diameter of recrystallized grains at the end of the process is given in Table 3, which compares the simulated and experimental values. Again, the model reproduces behavior expected based on experimental investigations: the average grain size generated at the end of primary recrystallization is independent of the treatment

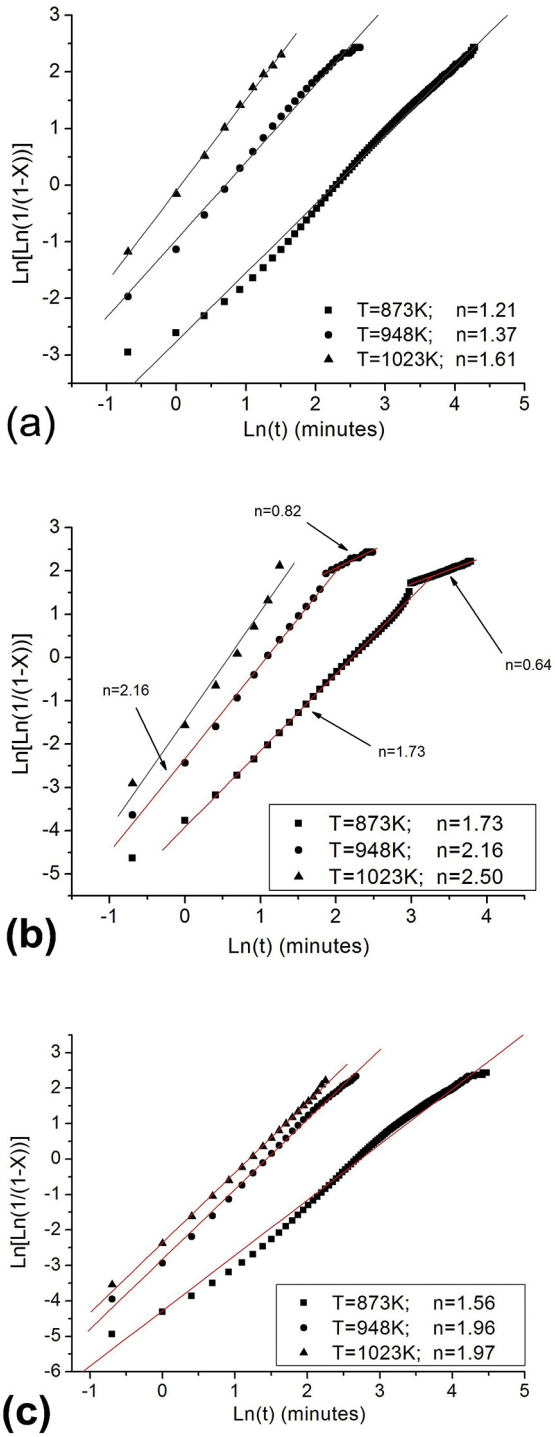

Figure 3: Avrami plots for temperatures 873 K, 948 K and 1023 K, from kinetics simulated by nucleation mechanisms of: site saturation (a), constant rate (independent of annealing temperature) (b) and temperature-dependent rate (c).

temperature[27,29]. According to Table 3, the difference between the experimental and simulated average grain size is small and lies within the margin of error. This also suggests that the spatial scaling proposed here is suitable for the simulated conditions. In these simulations, the average diameter of recrystallized grains is not only independent of the annealing temperature but also shows no significant differences between the nucleation mechanisms with rates that are temperature dependent and independent.

4.2 Grain growth

The grain growth step was simulated based on the microstructure generated by the model of primary recrystallization in which the nucleation rate is dependent on the annealing temperature, since the analysis of previous results indicated that this mechanism is the one that best describes the phenomenon in light of experimental results. It is worth noting that in the grain growth stage, the CAS/time ratio adopted equals 1.

Figure 5 presents graphs of the logarithm of average grain size as a function of the logarithm of time for each temperature considered. As expected, the rate of grain growth that characterizes the phenomenon's kinetics, as well as its average diameter, increases along with increasing temperature. The values of the growth exponent "m" obtained experimentally at each temperature are 0.58 for T = 873 K; 0.55 for T = 948 K and 0.50 for T = 1023 K[21]. Compared to the corresponding values resulting from the simulation presented in Figure 5, the percent difference among these values ranges from 10% to 29%. These differences are due, in part, to the relatively high experimental error in the grain size measurements, but do not constitute a serious discrepancy between the results of the model and the phenomenon evaluated experimentally.

Table 4 compares the simulated and experimental average grain diameters at 60, 120 and 240 minutes obtained at each temperature, indicating a good agreement between them.

Figure 6 depicts the simulated microstructures in the stage of grain growth after 1 and 4 hours at temperatures of 873 K and 1023 K. The grain morphology in the matrix is essentially equiaxial, characterizing a single-phase material with no preferential orientation for interface advance among grains and with minimization of the energy associated with the boundary, which is the dominant driving force in the growth process. Figure 7 compares the simulated and experimental microstructures obtained at 948 K after 60 and 240 minutes.

Figure 8 (a) shows the grain size distribution over time at the temperature of 948 K. At 60 minutes most of the grains are concentrated below 50 μm^2. Over time, there is a tendency for larger grains to grow while smaller grains gradually disappear, thereby changing the position of the maximum distribution to values between 50 μm^2 and 100 μm^2. Figure 8 (b) shows that the grain size distribution does not vary significantly over time, maintaining a constant standard deviation, thus characterizing normal growth. This behavior was expected since the model considers an initial matrix without deformation heterogeneities and without a predefined preferred orientation.

Table 2: Experimental and simulated results for primary recrystallization times of CP titanium, at each considered temperature and for each nucleation mechanism.

	Recrystallization time (min.)			
T (K)	saturation of sites	rate independent of temperature	rate dependent of temperature	experimental[21]
873	33.0±0.5	20.0±0.5	38.0±0.5	30±1
948	6.0±0.5	9.0±0.5	11.5±0.5	15±1
1023	3.0±0.5	3.5±0.5	7.5±0.5	7±1

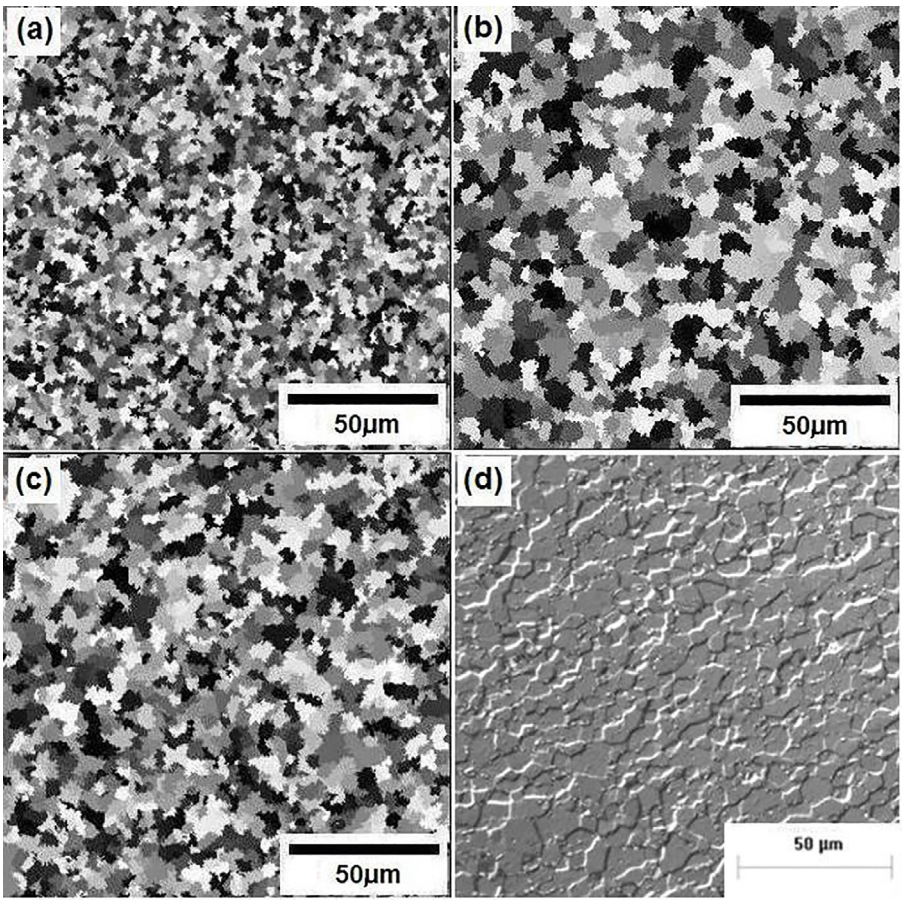

Figure 4: Microstructures at the end of primary recrystallization at 948 K: generated by simulation of these nucleation mechanisms: site saturation (a), rate independent of annealing temperature (b), annealing temperature-dependent rate (c), and rate obtained experimentally (d) in[21].

Table 3: Comparison of simulated and experimental results for the average diameter of recrystallized grains at the end of primary recrystallization, at each temperature and for each nucleation mechanism.

	Average diameter of recrystallized grains (µm)			
T(K)	saturation of sites	rate independent of temperature	rate dependent of temperature	experimental[21]
873	5±1	8±1	7±1	
948	5±1	8±1	7±1	8±2
1023	5±1	8±1	7±1	

4.3 Non-isothermal recrystallization

The model can also be used to simulate non-isothermal situations, extending directly to consider the variable temperature in each CAS time interval. A typical situation in which this adaptation can be tested is the simulation of differential scanning calorimetry (DSC) experiments. Such experiments can be performed to detect the occurrence of primary recrystallization, determine the material recrystallization temperature and evaluate the activation energy involved in

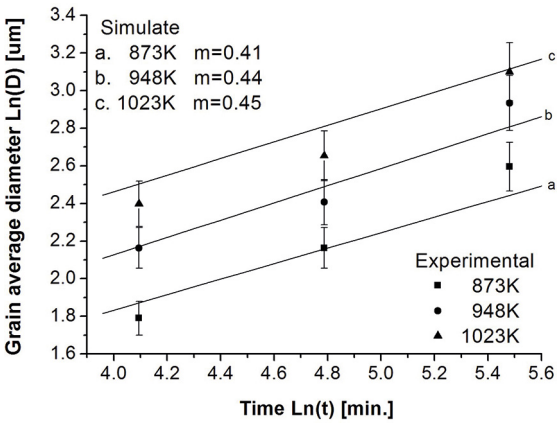

Figure 5: Temporal evolution of average grain diameter during growth at each isothermal treatment temperature.

the process[28]. Figure 9 illustrates the results for the simulation of the primary recrystallization kinetics occurring at heating rates of 5, 15 and 25 K/min. These rates are the same as those used in DSC experiments, with highly cold-worked samples of commercially pure titanium, which enabled the determination of activation energy and recrystallization temperature for the system under such conditions[21].

The analysis of Figure 9 indicates that the model of the nucleation mechanism whose rate is temperature-dependent yields results that are closer to the experimental data. The recrystallization temperature as a function of the imposed heating rate obtained by simulation lies in the range of 919 K and 960 K, while the temperature determined experimentally ranges from 917 K to 942 K[21], with a relative error of less than 4% between them. In addition, due to the fact that for non-isothermal conditions there is a dependence of temperature on the nucleation mechanisms, the driving force and growth rate became non-constant. That way, in according to previous discussions and also to observed at figure 9, the results are closer to the experimental data.

The recrystallization times in this non-isothermal process can be evaluated by analyzing Figure 9. Table 5 compares the recrystallization times estimated by simulation with those determined from the experimental curves for nucleation at a temperature-dependent rate and for each heating rate imposed on the system.

Figure 10 shows the simulated microstructures at the end of primary recrystallization in the condition in which the temperature is 15 K/min. Similarly to the case of recrystallization in the isothermal treatment, the average recrystallized grain diameter is lower in the mechanism of site-saturation nucleation, emphasizing the influence of the nucleation mechanism on the final average grain size. Morphologically, the structure shows equiaxed grains throughout the matrix.

5. Conclusions

This paper proposes a model to simulate primary recrystallization and grain growth phenomena under isothermal and non-isothermal conditions. The model is implemented computationally through a cellular automata algorithm. The simulated system corresponds to highly cold-worked CP-Ti grade 2, samples of which were subjected to isothermal treatments or to DSC tests in which a heating rate was imposed on the samples.

In the primary recrystallization stage under isothermal conditions, three possible simulation mechanisms are considered for the nucleation of new crystalline grains: site saturation nucleation, temperature-independent nucleation rate, and temperature-dependent nucleation rate. The recrystallization time and temperature dependence, average grain diameter and grain morphology at the end of primary recrystallization were determined for each of these mechanisms. A comparison of the simulated and experimental results for the system in question indicates that the mode that best simulates the phenomenon is the temperature-dependent nucleation rate and that the spatial and temporal scaling suggested in the algorithm is suitable. Observing the Avrami curves, it is possible to note deviations from the predictions of JMAK theory which are indicated by changes in the Avrami exponent in the final moments of primary recrystallization. This finding is consistent with those of other studies reported in the literature, both experimental and theoretical.

Based on the microstructure obtained at the end of primary recrystallization, the nucleation mechanism at a temperature-dependent rate follows the simulation of the stage of grain growth in isothermal treatments. It appears that temperature increases tend to increase the growth exponent, and the difference between the growth exponents resulting from the simulations and their respective experimental values is between 10% and 29%. The simulated average grain diameter and the corresponding experimental values are in good agreement,

Table 4: Average grain diameters obtained in the simulation, in microns, compared with the experimental values obtained after 60, 120 and 240 minutes at each heat treatment temperature.

	Average diameter of grains (μm)								
	873K			948K			1023K		
	60 min.	120 min.	240 min.	60 min.	120 min.	240 min.	60 min.	120 min.	240 min.
Simulated	7±1	8±1	10±1	8±1	10±1	15±1	13±1	20±1	27±1
Experimental[21]	5±2	8±2	13±2	8±2	11±2	18±2	11±2	14±2	22±2

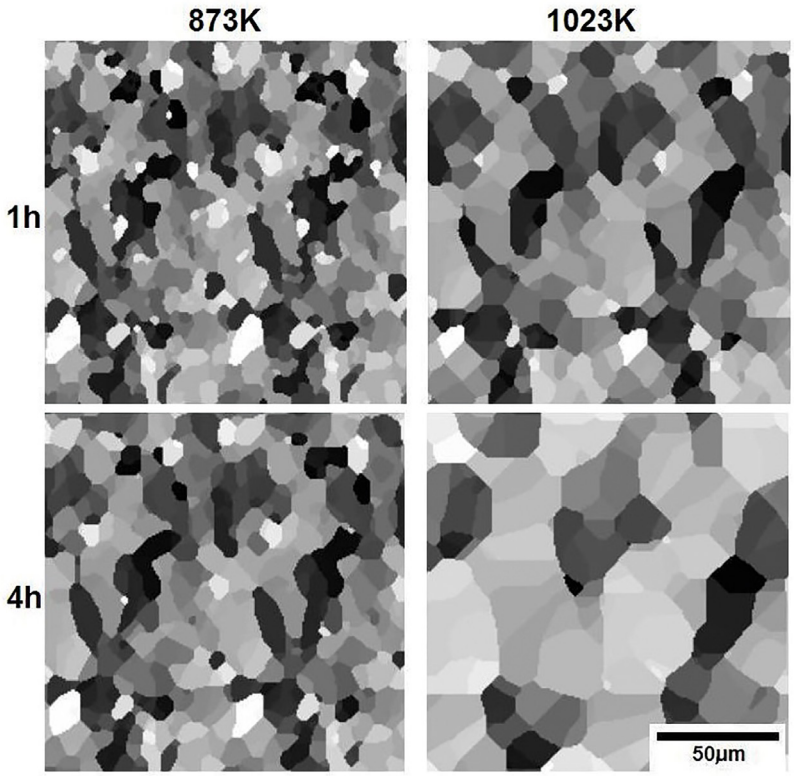

Figure 6: Evolution of grain structure simulated at temperatures of 873 K and 1023 K after 60 and 240 minutes.

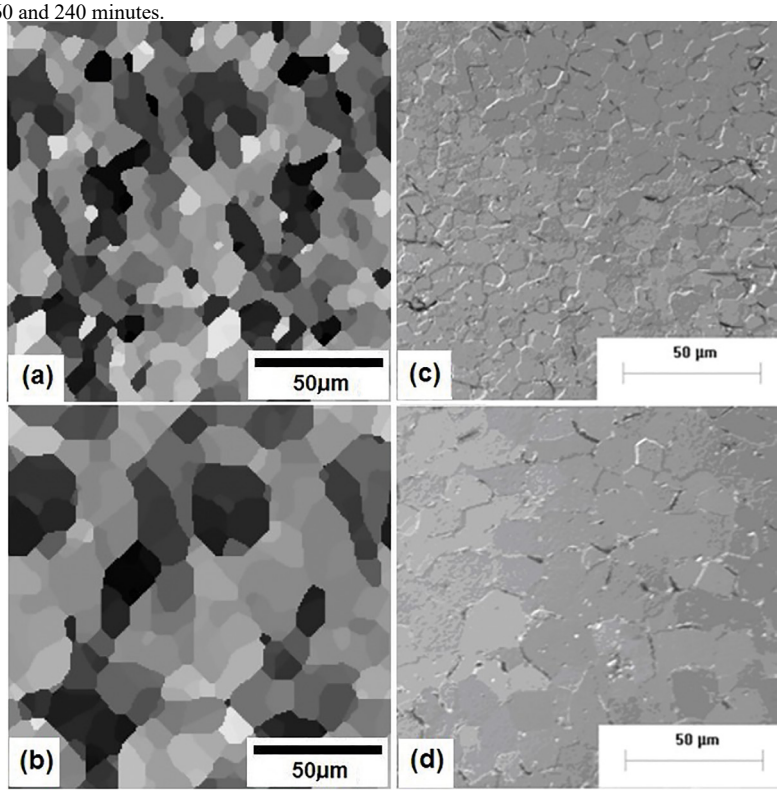

Figure 7: Temporal evolution of grain structure at a temperature of 948 K after 60 and 240 minutes: (a) and (b) simulated, (c) and (d) micrographs of grain structure obtained experimentally[21].

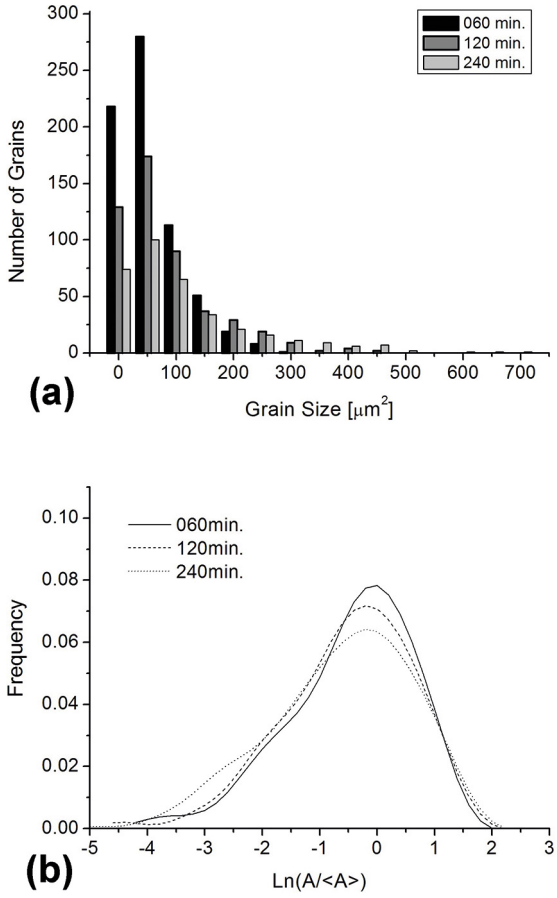

Figure 8: (a) Distribution of average grain size after 60, 120 and 240 minutes at a temperature of 948 K. (b) Normalized distribution.

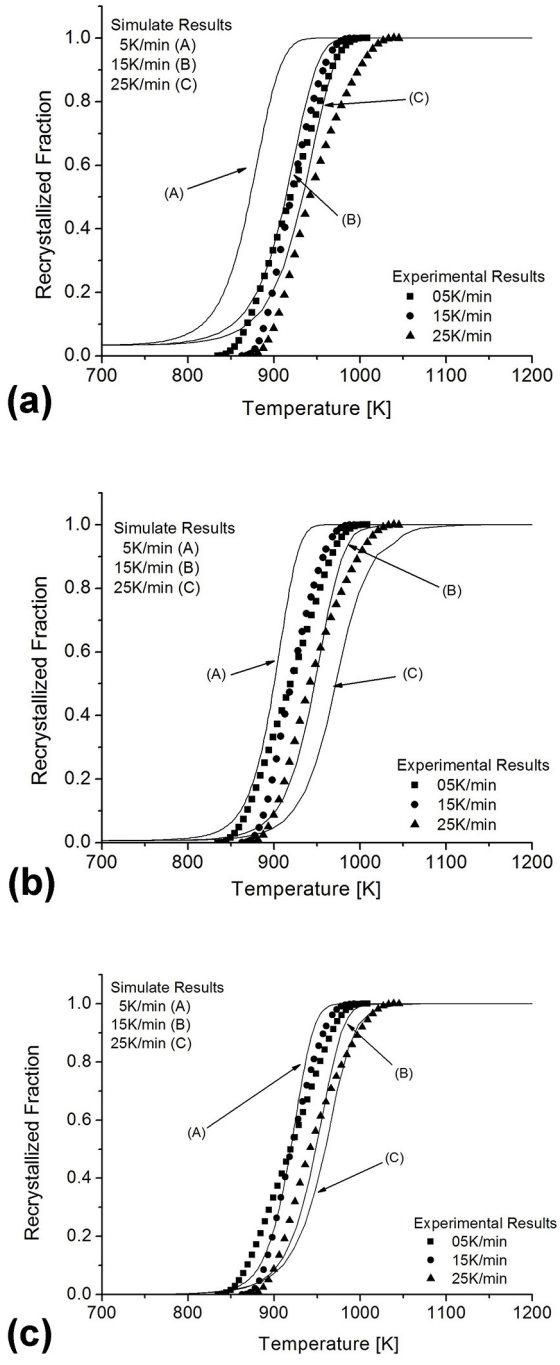

Figure 9: Evolution of the recrystallized fraction as a function of temperature for the nucleation mechanisms of: (a) site saturation, (b) temperature-independent rate, and (c) temperature-dependent rate.

with the simulated structure composed of grains in the process of equiaxed growth. The grain size distribution indicates the occurrence of normal grain growth during the simulation.

Extending the code to include situations in which the temperature varies over time allows for the simulation of recrystallization in samples subjected to DSC tests at predetermined heating rates. Again, the results that best corresponded to the experimental data for the kinetics of transformation in CP-Ti were obtained with the temperature-dependent nucleation mechanism. The relative error between the recrystallization temperatures calculated in the simulation and that obtained from the DSC experimental curve was lower than 4%.

With a proper calibration of the spatial and temporal scales and the insertion of fundamental physical characteristics of the processes into the model, such as the nucleation mechanisms and the principle of minimum energy, cellular automata algorithms can be used in quantitative simulations of primary recrystallization and grain growth in isothermal and non-isothermal conditions.

Table 5: Evaluation of the recrystallization times, in minutes, based on the simulated and experimental curves in Figure 9 (c), at each heating rate.

Heating rate (K/min)	Simulated time (min)	Experimental time (min)
5	22.0±0.5	27.0±0.5
15	8.7±0.5	6.7±0.5
25	6.4±0.5	5.8±0.5

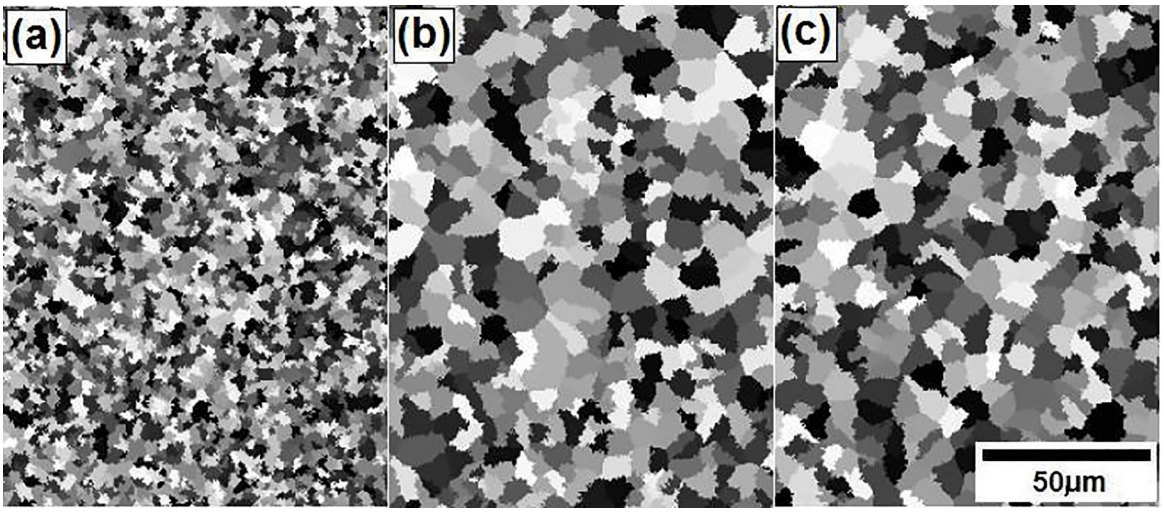

Figure 10: Microstructures generated by non-isothermal simulation at heating rates of 15 K/minute from the nucleation mechanisms of (a) site saturation, (b) temperature-independent rate, and (c) temperature-dependent rate.

6. Acknowledgments

The authors gratefully acknowledge the Brazilian research funding agencies FAPESP (State of São Paulo Research Foundation) and CNPq (National Council for Scientific and Technological Development) for their financial support of this work.

7. References

1. Madej L, Sitko M, Randwanski K, Kuziak R. Validation and predictions of coupled finite element and cellular automata model: Influence of the degree of deformation on static recrystallization kinetics case study. *Materials Chemistry and Physics*. 2016;179:282-294.

2. Sitko M, Pietrzak M, Madej L. Time and legth scale issues in numerical modelling of dynamic recrystallization based on the multi space cellular automata method. *Journal of Computational Science*. 2016;16:98-113.

3. Toffoli T. Cellular automata as an alternative to (rather than an approximation of) differential equations in modeling physics. *Physica D: Nonlinear Phenomena*. 1984;10(1-2):117-127.

4. Raabe D. Cellular Automata in Materials Science with Particular Reference to Recrystallization Simulation. *Annual Review of Materials Research*. 2002;32:53-76.

5. Hesselbarth HW, Göbel IR. Simulation of recrystallization by cellular automata. *Acta Metallurgica et Materialia*. 1991;39(9):2135-2143.

6. Davies CHJ. Growth of nuclei in a cellular automaton simulation of recrystallization. *Scripta Materialia*. 1997;36(1):35-40.

7. Kugler G, Turk R. Study of the influence of initial microstructure topology on the kinetics of static recrystallization using a cellular automata model. *Computational Materials Science*. 2006;37(3):284-291.

8. Ghosh S, Gabane P, Bose A, Chakraborti N. Modeling of recrystallization in cold rolled copper using inverse cellular automata and genetic algorithms. *Computational Materials Science*. 2009;45(1):96-103.

9. Rios PR, Jardim D, Assis WLS, Salazar TC, Villa E. Inhomogeneous Poisson point process nucleation: comparison of analytical solution with cellular automata simulation. *Materials Research*. 2009;12(2):219-224.

10. Goetz RL, Seetharaman V. Modeling Dynamic Recrystallization Using Cellular Automata. *Scripta Materialia*. 1998;38(3):405-413.

11. Qian M, Guo ZX. Cellular automata simulation of microstructural evolution during dynamic recrystallization of an HY-100 steel. *Materials Science and Engineering: A*. 2004;365(1-2):180-185.

12. Ding R, Guo ZX. Coupled quantitative simulation of microstructural evolution and plastic flow during dynamic recrystallization. *Acta Materialia*. 2001;49(16):3163-3175.

13. Yazdipour N, Davies CHJ, Hodgson PD. Microstructural modeling of dynamic recrystallization using irregular cellular automata. *Computational Materials Science*. 2008;44(2):566-576.

14. Geiger J, Roósz A, Barkóczy P. Simulation of grain coarsening in two dimensions by cellular-automaton. *Acta Materialia*. 2001;49(4):623-629.

15. He Y, Ding H, Liu L, Shin K. Computer simulation of 2D grain growth using a cellular automata model based on the lowest energy principle. *Materials Science and Engineering: A*. 2006;429(1-2):236-246.

16. Ding HL, He YZ, Liu LF, Ding WJ. Cellular automata simulation of grain growth in three dimensions based on the lowest-energy principle. *Journal of Crystal Growth*. 2006;293(2):489-497.

17. Raghavan S, Sahay SS. Modeling the grain growth kinetics by cellular automaton. *Materials Science and Engineering: A*. 2007;446-446:203-209.

18. Rappaz M, Gandin CA. Probabilistic modelling of microstructure formation in solidification processes. *Acta Metallurgica et Materialia*. 1993;41(2):345-360.

19. Nastac L, Stefanescu DM. Stochastic modelling of microstructure formation in solidification processes. *Modelling and Simulation in Materials Science and Engineering*. 1997;5(4):391-420.

20. Zhu MF, Hong CP. Modeling of microstructure evolution in regular eutectic growth. *Physical Review B*. 2002;66(15):155428.

21. Contieri RJ, Zanotello M, Caram R. Recrystallization and grain growth in highly cold worked CP-Titanium. *Materials Science and Engineering: A*. 2010;527(16-17):3994-4000.

22. Gottstein G. *Physical Foundations of Materials Science*. Berlin Heidelberg: Springer-Verlag; 2004.

23. Thiessen RG, Richardson IM. A physically based model for microstructure development in a macroscopic heat-affected zone: Grain growth and recrystallization. *Metallurgical and Materials Transactions B*. 2006;37(4):655-663.

24. Wolf D. A Read-shockley model for high-angle grain boundaries. *Scripta Metallurgica*. 1989;23(10):1713-1718.

25. Chun YB, Semiatin LS, Hwang SK. Monte Carlo modeling of microstructure evolution during the static recrystallization of cold-rolled, commercial-purity titanium. *Acta Materialia*. 2006;54(14):3673-3689.

26. Kugler G, Turk R. Modeling the dynamic recrystallization under multi-stage hot deformation. *Acta Materialia*. 2004;52(15):4659-4668.

27. Padilha AF, Siciliano Jr. F. *Encruamento, recristalização, crescimento de grão e textura*. São Paulo: Associação Brasileira de Metalurgia e Materiais; 2005.

28. Benchabane G, Boumerzoug Z, Thibon I, Gloriant T. Recrystallization of pure copper investigated by calorimetry and microhardness. *Materials Characterization*. 2008;59(10):1425-1428.

29. Timoshenkov A, Warczok P, Albu M, Klarner J, Kozeschnik E, Bureau R, et al. Modelling the dynamic recrystallization in C–Mn micro-alloyed steel during thermo-mechanical treatment using cellular automata. *Computational Materials Science*. 2014;94:85-94.

30. Rios PR, Siciliano Jr F, Sandim HRZ, Plaut RL, Padilha AF. Nucleation and growth during recrystallization. *Materials Research*. 2005;8(3):225-238.

31. Poorganji B, Sepehrband P, Jin H, Esmaeili S. Effect of cold work and non-isothermal anneling on the recrystallization behavior and texture evolution of a precipitation-hardenable aluminum alloy. *Scripta Materialia*. 2010;63(12):1157-1160.

32. Janssens KGF. Random grid, three-dimensional, space-time coupled cellular automata for the simulation of recrystallization and grain growth. *Modelling and Simulation in Materials Science and Engineering*. 2003;11(2):157.

33. Anderson MP, Srolovitz DJ, Grest GS, Sahni PS. Computer simulation of grain growth—I. Kinetics. *Acta Metallurgica*. 1984;32(5):783-791.